

EMISSION-LINE DIAGNOSTICS OF GALAXY EVOLUTION WITH NGST

R.C. Kennicutt

Steward Observatory, The University of Arizona, Tucson, AZ 85721, USA
Tel: 520-621-4032; FAX: 520-621-1532; Email: rkennicutt@as.arizona.edu

ABSTRACT

As a byproduct of its search for the first star forming galaxies, NGST will obtain high-quality spectra for thousands of galaxies in the redshift range $z = 0 - 6$ and beyond. Most of the galaxies will possess strong emission-line spectra, and these spectra will provide a wealth of quantitative information on their star formation rates, reddening, metal abundances, internal kinematics, and nuclear activity. This will make it possible to construct a comprehensive picture of the buildup of stars, metals, dust, and the nuclei of galaxies with cosmological lookback time. This paper reviews what can be learned from the spectra of distant emission-line galaxies. Simulations of NGST spectra are used to explore the instrumental trade-offs for these applications, and the respective roles of NGST and groundbased surveys.

Key words: NGST; galaxy evolution; spectroscopy.

1. INTRODUCTION

One of the most important themes to emerge from this conference has been that NGST, besides fulfilling its core goal of identifying the first stars and galaxies, has the extraordinary potential to trace the *physical* evolution of galaxies over the redshift range $z = 0 - 6$ and higher (see the other papers in this volume by Dressler, Ellis, Stiavelli, and White). The deep surveys with NGST will produce spectra for thousands of galaxies, and these spectra will contain quantitative information on the star formation rates (SFRs), reddening and extinction, metal abundances, kinematics, and nuclear properties for most of these objects. This will provide a comprehensive inventory of the buildup of stars, metals, dust, mass, and the nuclei of galaxies over lookback times ranging from a billion years after the Big Bang to the present. This goldmine of information may well prove to be among the chief scientific achievements of NGST.

This lofty objective is achievable because NGST can provide high-S/N spectra of the complete visible and near-infrared spectral regime, out to redshifts of at least $z = 6$, thus making it possible to apply the array of nebular diagnostic methods that have been developed for groundbased studies of nearby galaxies. As

an illustration of NGST's unique potential, Figure 1 shows a simulated NGST observation of the prototypical nuclear starburst galaxy NGC 7714, observed at a redshift $z = 6$ (see Sec. 3 for a discussion of the simulation parameters). The combination of high spatial resolution, low background, and continuous spectral coverage will make it possible to use spectra like these to derive hard numbers on SFRs, dust content, metal abundances, and nuclear emission properties for the emission-line galaxies that comprise the dominant population at $z > 1$.

The goal of this paper is to review the diagnostic methods that can be applied to the integrated emission-line spectra of galaxies, and to explore the potential application of these techniques with NGST. I begin by discussing the astrophysical parameters that can be extracted from emission-line spectra, and the corresponding instrumental requirements in wavelength coverage, resolution, and S/N. I then present some examples of simulated NGST spectra, derived using the baseline parameters in the NGST

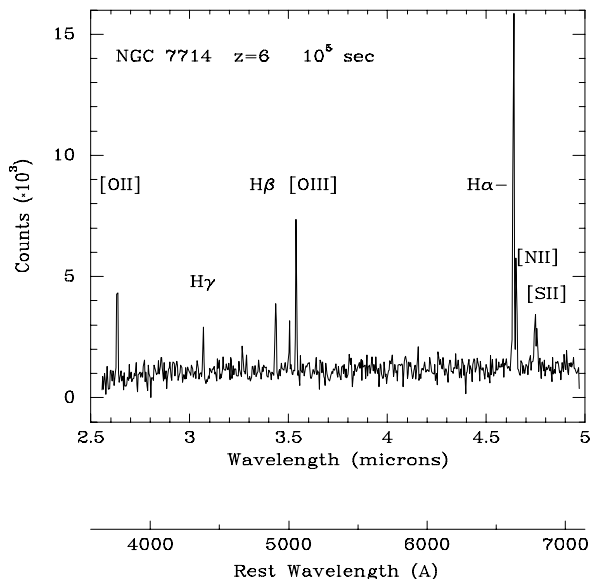


Figure 1. Simulated NGST spectrum of the nearby starburst galaxy NGC 7714, observed at redshift $z = 6$. The bottom axes show both observed (redshifted) and rest wavelengths, with the principal spectral features labeled.

Table 1. Summary of emission-line diagnostics.

Parameter	Features	Resolution	S/N ($H\alpha$)
SFRs	$H\alpha$, ([OII], $H\beta$)	100–300	>10
Reddening/Extinction	$H\alpha$, $H\beta$	500–2000	>20
Metal Abundance	$H\beta$, [OIII], [OII], ($H\alpha$, [NII], [SIII])	300–1000	>10
AGN Diagnostics	$H\beta$, [OIII], [NII], [SII], ([OI])	500–2000	>20
Kinematics	$H\alpha$, ([OII])	1000–10000	>10–20

yardstick design in the NGST “black book” (Stockman 1997). These provide useful insight into the ranges of spectral resolutions and integration times that are needed for these applications, and they clearly illustrate the complementary roles that will be played by NGST and future groundbased surveys. My discussion is intended to complement the paper by Stiavelli presented elsewhere in this volume. In order to limit the scope of my presentation I have emphasized applications of moderate-resolution ($R \leq 2000$) visible emission-line spectroscopy, and I will say relatively little about the potentially important applications of absorption-line spectra or near-infrared emission-line spectroscopy.

2. EMISSION-LINE DIAGNOSTICS OF GALAXY EVOLUTION

Figure 1 shows the principal nebular lines that are available in the redshifted visible range. The dominant features are recombination lines of hydrogen ($H\alpha$, $H\beta$, $H\gamma$) and helium (mainly He I 5876), and forbidden lines of [OII] λ 3726,3729, [OIII] λ 4959,5007, [NII] λ 6548,6583, and [SII] λ 6717,6731. These lines by themselves provide a diverse array of diagnostics of SFRs, reddening, abundances, velocity fields, and nuclear emission properties. Because they span less than an octave in wavelength the entire set of lines can be observed in the 1–5 μ m window over a wide redshift range ($z = 1.7 - 6.4$). Much of the diagnostic information is contained in lines with wavelengths of 3727–5007 Å, and this range is accessible shortward of 5 μ m out to $z \sim 9$. Other useful visible-wavelength features include the shock and AGN-sensitive [OI] λ 6300,6363 doublet, and the temperature-sensitive auroral line of [OIII] λ 4363. However in most star forming galaxies these features have fluxes of only a few percent of $H\alpha$ or less, and will only be seen in very high S/N spectra. The rest near-infrared region contains a number of other potentially valuable diagnostic features, including the Paschen and Brackett recombination lines (extremely valuable for measuring SFRs in dusty regions), the ionization-sensitive [SIII] λ 9069,9532 doublet, the shock-sensitive [FeII] lines longward of 1.2 μ m, and several diagnostics of molecular and coronal-phase gas. These features will be redshifted into the zodiacal background for high-redshift objects, but will provide valuable diagnostic information for

intermediate-redshift galaxies.

Table 1 presents a summary of the observational requirements for some of the main nebular diagnostics. In each case I list the relevant emission lines, and the approximate ranges of spectral resolution and S/N required, with higher values indicating the optimal desirable performance, and the lower values indicating what I regard as the minimal capability needed for quantitative applications. I briefly discuss each application individually below. Since observations of galaxy kinematics are dealt with extensively in other papers, I will not discuss that application further here.

2.1. Star Formation Rates

The $H\alpha$ luminosity of a galaxy provides a robust measure of its global SFR, which is directly tied to the luminosity and mass of the young massive stellar population (Kennicutt 1983, 1998). $H\alpha$ data provide most of our information on the systematics of SFRs in nearby galaxies, but the redshifting of $H\alpha$ outside the visible window for $z \geq 0.5$ has hampered its application to high-redshift galaxies. Instead, most of what is known about the cosmic evolution of the SFR comes from redshifted UV continuum measurements (e.g., Madau et al. 1996), supplemented to some extent by [OII] emission-line observations (e.g., Cowie et al. 1997). As discussed at this conference by Madau and others, large uncertainties in the extinction corrections in the UV continuum measurements introduce uncertainty into both the normalization and shape of the Madau diagram. NGST will be capable of detecting $H\alpha$ directly out to $z \sim 7$, with reddening information available from the Balmer decrement (below). This will provide independent measures of the SFR, and a solid cross-check on the cosmic evolution of the SFR determined from other methods.

The $H\alpha$ line is usually among the strongest emission features in the integrated spectra of galaxies, so this application can be accommodated with relatively modest spectral resolution and S/N. Figure 2 shows examples of moderate-resolution ($R = 800$) integrated spectra for 4 nearby galaxies from the atlas of Kennicutt (1992b), chosen to span the range of SFRs observed in local spiral and irregular galaxies. A minimum resolution is set by the need to resolve

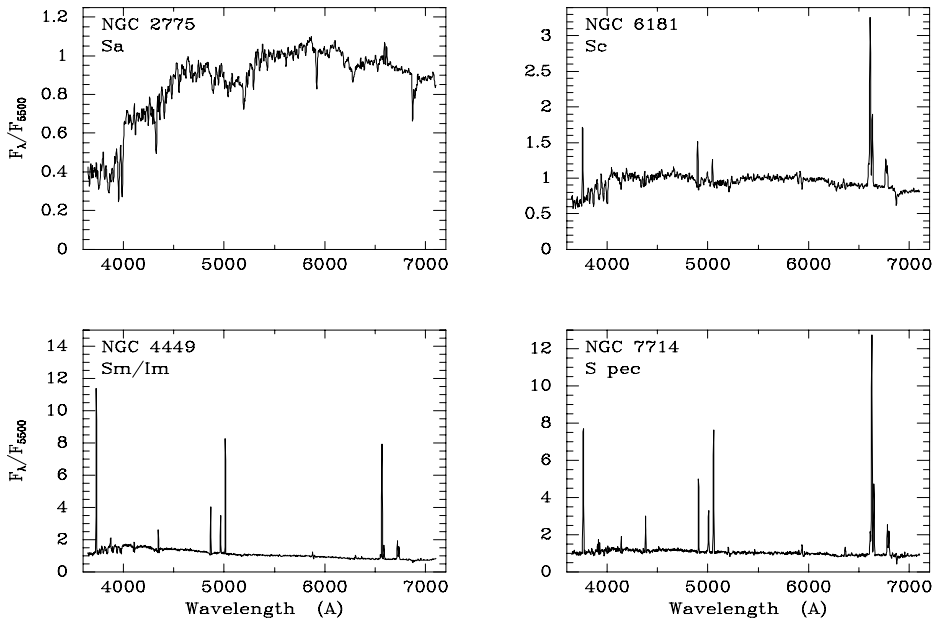


Figure 2. Integrated spectra of 4 nearby spiral and irregular galaxies, from the sample of Kennicutt (1992b).

$H\alpha$ from the [NII] λ 6583 line ($R \geq 400$), but useful information on the SFR can be obtained even with resolutions of order 100 and S/N of ~ 10 .

Exploratory studies of the redshifted $H\alpha$ emission of distant galaxies are already being carried out from the ground (e.g., Bechtold et al. 1997), and several large surveys are being planned for groundbased spectrographs on 8–10 m class telescopes. The main limitation in these studies is not sensitivity but rather interference from the telluric OH emission in the 0.8–2 μ m region, and the steeply rising thermal background longward of 2 μ m. It is likely that $H\alpha$ -determined SFRs will have been measured for thousands of galaxies out to $z \sim 2$ in the next decade, as well as for a smaller number of luminous objects at higher redshifts. The main value of NGST will be in extending the application to higher redshifts, and in obtaining SFRs for complete samples over the full redshift range.

In applications where $H\alpha$ is unobservable it is possible to use the higher-order Balmer lines (e.g., $H\beta$) or even a forbidden line such as [OII] λ 3727 as a substitute SFR measure. The $H\beta$ line is useful in galaxies with sufficiently strong emission so that the effects of underlying stellar absorption are small. This condition is satisfied in local emission-line starburst galaxies, but not among normal disk galaxies or post-burst galaxies (Kennicutt 1992a). Several workers have used the [OII] line to estimate the evolution in the SFR with redshift (e.g., Cowie et al. 1997). The advantages of [OII] are its relative strength and its observability to much higher redshifts than $H\alpha$. However the strength of the line is not directly tied to the photoionization rate; the ratio of the line flux to the SFR is sensitive to excitation variations as well as to reddening. This ratio can easily vary by a full order of magnitude in luminous spiral galaxies (Kennicutt 1992a), but it appears to be a more reliable measure of the SFR in strong emission-line galaxies (Gallagher et al. 1989, Jansen et al. private communication). Several large spectrophotometric surveys of nearby galaxies that are currently under

way should provide a firmer test of the reliability of [OII]-derived SFRs over the next few years. However the systematic changes in [OII] excitation with abundance, dust content, and ionization parameter remain a cause of some concern for lookback applications (Kennicutt 1992a, 1998), and whenever possible a SFR scale directly anchored on recombination lines is preferable.

2.2. Reddening and Extinction

As mentioned earlier, extinction remains as the largest single source of uncertainty in current studies of the evolution of the cosmic star formation rate. Nebular SFRs are hardly immune from extinction problems, but the nebular spectrum offers a means of constraining the reddening and extinction via the Balmer decrement. This requires considerably higher S/N spectra than for $H\alpha$ -based SFRs alone, ideally with sufficient spectral resolution and S/N to detect any stellar absorption under $H\beta$.

Spectra integrated over a large spatial region will tend to underestimate the total extinction, because the observed Balmer decrement will be weighted to the regions of lowest line-of-sight extinction. However studies of nearby starbursts and disk HII regions suggest that the reddening measured by the Balmer decrement can provide a reasonable estimate of the visible and UV extinction (e.g., Calzetti et al. 1994, Buat & Xu 1996).

One regime in which the visible measurements break down entirely is in the dusty cores of luminous infrared starburst galaxies. Most of these objects show a pronounced emission-line spectrum in the visible, but the nebular reddening may bear little relation to the extinction, which often amounts to several magnitudes in the visible. Such objects may represent a substantial component of the high-redshift starburst population, and thus it is important to supplement any survey of the redshifted UV–visible spectra with

coordinated observations of the redshifted infrared emission. In cases where the Paschen lines are detectable with NGST they would provide a critical test of the reliability of the $H\alpha$ and UV-derived SFRs.

2.3. Metal Abundances

One of the most exciting prospects for NGST spectroscopy is the determination of gas-phase metal abundances for high- z galaxies. As discussed in the review by Stiavelli, a rigorous determination of the nebular oxygen abundance requires an accurate measurement of the temperature-sensitive [OIII] λ 4363 line or another auroral line. However the flux of this line is typically of order 0.1–1% of [OIII] λ 4959,5007, so direct abundance determinations will be limited to the brightest galaxies, and those with relatively weak stellar continuum.

Most determinations of abundances in high- z galaxies will probably be based on the empirically-calibrated strong-line indices, for example the widely applied R_{23} index of Edmunds & Pagel (1984):

$$R_{23} \equiv \frac{[OII]\lambda 3726, 3729 + [OIII]\lambda 4959, 5007}{H\beta} \quad (1)$$

For metal abundances $Z \geq 0.2Z_{\odot}$ the relationship between R_{23} and oxygen abundance is monotonic, with the forbidden lines becoming *weaker* with increasing abundance. The index has been calibrated using a combination of observed abundances (calibrated with [OIII] λ 4363 measurements) and nebular models for the most metal-rich regions (e.g., McGaugh 1991). Over the abundance range of about $0.2 Z_{\odot} < Z < Z_{\odot}$ the R_{23} index can provide HII region abundances that are accurate to within about ± 0.1 – 0.2 dex, with somewhat larger errors at higher abundances, where the calibration rests almost entirely on models. The method has been widely applied to HII region surveys of nearby galaxies (e.g., Zaritsky et al. 1994), and in principle should be applicable to high- z objects. Kobulnicky & Zaritsky (1998) have used Keck spectroscopy of a sample of galaxies at $z = 0.1 - 0.5$ to test this technique, and to explore the physical nature of the compact narrow emission-line galaxies that are frequently observed at these redshifts (e.g., Koo et al. 1995). The abundances measured for these objects, typically in the range 0.2 – $1.5 Z_{\odot}$, already rule out a popular interpretation of these objects as progenitors to present-day dwarf spheroidal galaxies. This illustrates the potential power of abundance measurements for constraining the physical evolution of high-redshift objects, especially if the data can be combined with measurements of their luminosities, velocity dispersions, SFRs, and other properties.

A major concern for the application of these methods to distant galaxies is the effect of beam smearing on the integrated line ratios. The strengths of the [OII] and [OIII] lines follow well-defined but nonlinear dependences on abundance, and it is not at all clear *a priori* whether the nebular excitation inferred from a large spatial region— with contributions from several regions with possibly different abundances and

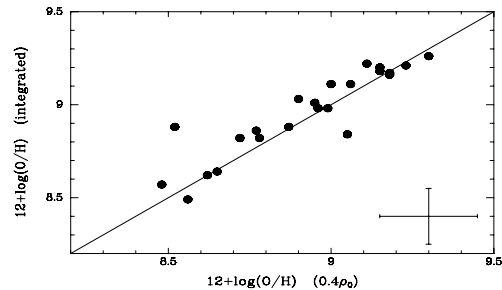


Figure 3. Comparison of oxygen abundances inferred from the integrated emission-line spectra of disks, using the R_{23} method, and the actual abundance at $0.4 R_0$, from the study of Kobulnicky et al. (1998).

ionization properties— will necessarily correlate with the mean abundance in the same way as for individual HII regions. I have investigated this recently in collaboration with Chip Kobulnicky and James Pizagno (Kobulnicky et al. 1998). We combined published HII region spectra of a large sample of galaxies with well-measured abundance distributions with radial $H\alpha$ emission profiles, to simulate the integrated emission-line spectra of the galaxies. We then compared the abundance one would infer from the integrated R_{23} ratio with the actual abundance measured for the disk. Figure 3 shows the comparison, with the integrated measurement compared in this case to the observed abundance at $0.4 R_0$. There is an excellent correlation, with only one pronounced outlier (M101), a galaxy with an unusually extended star forming disk and an unusually strong abundance gradient. This comparison suggests that the sampling error in determining mean abundances from the integrated spectra is comparable to or smaller than the intrinsic error in the R_{23} method itself, so comparisons like those carried out by Kobulnicky & Zaritsky (1998) should be valid. The comparison shown in Figure 3 does not include the contribution of diffuse ionized gas to the integrated spectrum, but observations by Hunter (1994) and Martin (1997) suggest that while the relative strengths of [OII] and [OIII] can be quite different from those of normal HII regions, the R_{23} values roughly follow the same abundance relation to first order. We have also investigated the effects of beam smearing on spectra with detectable [OIII] λ 4363, using measured longslit spectra of nearby galaxies. There is evidence for a systematic bias toward lower inferred abundances, but the effect is small (~ 0.1 dex), and consistent enough that a correction for this effect can be applied.

This technique is already being applied from the ground, for low-redshift galaxies in the visible (e.g., Kobulnicky & Zaritsky 1998) and for $z \simeq 3$ galaxies in the infrared (e.g., Pettini et al. 1998). It is likely that such measurements will be carried out for large samples of galaxies before NGST is launched. However the groundbased observations will be handicapped in several important respects. At a minimum, a reliable abundance measurement requires the measurement of at least three emission features ([OII] λ 3727, $H\beta$, and [OIII] λ 4959 or [OIII] λ 5007), and the probability of avoiding a strong telluric emission or absorption line quickly decreases as the number of lines increases. Equally serious is the break-

down in the R_{23} index below abundances of roughly $0.2 Z_{\odot}$. At very low abundances the forbidden-line strengths decrease with decreasing abundance, so R_{23} becomes a double-valued function of oxygen abundance, and there is a broad region between about $0.1\text{--}0.3 Z_{\odot}$ where R_{23} is roughly constant, and thus is completely insensitive to abundance. Unfortunately this is just in the range that one might expect many high-redshift galaxies to fall. One can circumvent this problem either by observing a temperature-sensitive line such as [OIII] λ 4363, or more realistically by combining the information on R_{23} with the ratio of [OII]/[OIII] and measurements of other lines such as [NII] λ 6583, [SII] λ 6717,6731, and/or [SIII] λ 9069,9532 (e.g., Skillman 1989). Obtaining spectra over such a wide spectral range will be problematic from the ground, but is feasible with NGST (see Figure 1).

The instrumental requirements for abundance measurements are similar to those for measuring SFRs and reddening, except that a broad simultaneous spectral coverage is desirable in this instance. A clean resolution of [NII] from H α is desirable, especially in low-metallicity objects where [NII] will be very weak. This implies spectral resolution $R \geq 500$ and S/N > 30 in the strongest lines. For more metal-rich objects the requirements are somewhat lower.

2.4. Nuclear Activity and Star Formation

Another area in which NGST should make major progress is in tracing the evolution of nuclear activity and star formation with lookback time. For most realistic cosmologies the angular resolution of NGST corresponds to linear scales of a few hundred parsecs (for all redshifts of interest), and galactic nuclei will be cleanly resolved in images and spectra. The same diagnostics as discussed in Sec. 2.1 can be used to measure the nuclear SFRs, and compare the cosmic evolution of the nuclear and global SFRs. The extensive wavelength coverage that is attainable with NGST will also make it possible to apply the familiar diagnostic lines ([OIII], [NII], [SII], [OI], [SIII]) to distinguish star forming nuclei from Seyfert nuclei, LINERs, and other AGN types (e.g., Veilleux & Osterbrock 1987).

This application has not been widely discussed in framing the science case for NGST, but I believe it represents an enormously rich opportunity. Spectroscopic observations of nearby galaxies suggest that massive nuclear black holes may be a ubiquitous phenomenon, at least among galaxies with large central spheroids. If this is the case, NGST offers us the opportunity to directly observe the buildup of these central mass concentrations, and extend the study of the frequency and luminosity evolution of nonthermal nuclear activity to a millionfold dynamic range in nuclear luminosity. All of these applications will be nearly impossible to duplicate from the ground.

The instrumental requirements closely match those for the abundance measurements, in cases where only the fluxes of emission lines are required. At resolutions $R \geq 1000$ and high S/N one can begin to use the nuclear line profiles as diagnostics as well.

3. PROSPECTS WITH NGST

The previous section outlined the astrophysical and instrumental wish lists for these applications. What are the prospects for meeting these with NGST? To address this question I have constructed simulations of spectroscopic observations with NGST, using integrated spectra of nearby galaxies from Kennicutt (1992b) and the artificial data package in IRAF. Slit spectra were constructed for selected galaxies observed at redshifts $z = 0 - 9$. I also used H α images of a few nearby galaxies to simulate 2D emission-line images in the NGST focal plane, in order to explore the effects of spatial sampling on the observability of distant galaxy spectra.

Table 2. Simulation parameters.

Cosmology	$H_0=75, \Omega_0=0.3, \Lambda_0=0$
Galaxy Luminosity	$M_B^* = -21.0$
NGST Aperture	$D = 8 \text{ m } (A = 50 \text{ m}^2)$
System Efficiency	0.2
Sky Background	$2 \times \text{DIRBE minimum}$
Instrumentation	
– pixel size	0.03 arcsec
– readout noise	$10 e^-$
– dark noise	$0.01 e^-/\text{sec/pixel}$
– integration time	1000 sec
Spectroscopy	
– slit width	0.1 arcsec
– slit length	$0.1\text{--}0.3 \text{ arcsec } (\sim 1\text{--}3 \text{ kpc})$
– resolution	$R = 800 (3 \text{ pixels})$

Table 2 lists the parameters and assumptions that were used in the simulations shown here. It is important to bear in mind that with so many uncertainties in the instrument design one can only approximate what might be expected with NGST, and in most respects I have attempted to be conservative in my assumptions. As discussed later, the most critical parameters are the detector noise figures, which in this case were taken from Stockman (1997). Almost all spectroscopic applications are detector noise limited, and this influences many of the observational parameters, in particular the optimal slit sampling and the integration times. For the parameters chosen, detector read noise and dark noise are significant contributors. In the $1\text{--}5 \mu\text{m}$ region the assumed sky background is typically less than 10% of the detector noise, and can be ignored for most applications (however the sky quickly dominates the noise longward of $5 \mu\text{m}$). To be conservative I have subtracted a background from each spectrum, which has the practical effect of increasing the net noise by a factor of 1.414.

As an illustration of the range of spectra that are likely to be seen with NGST, Figure 4 shows the same nearby galaxies as in Figure 2, but in this case observed at $z = 3$ with NGST, with spectral resolution $R = 800$ and a total integration time of 100 ksec. To facilitate the comparison the galaxy luminosities have been normalized to a common value of $M_B = -21$, but it is assumed that only 20% of this luminosity is contained in an aperture of 0.1×0.3 arcsec. Larger apertures would include more of the disks, but would degrade the S/N due to the larger number of detector

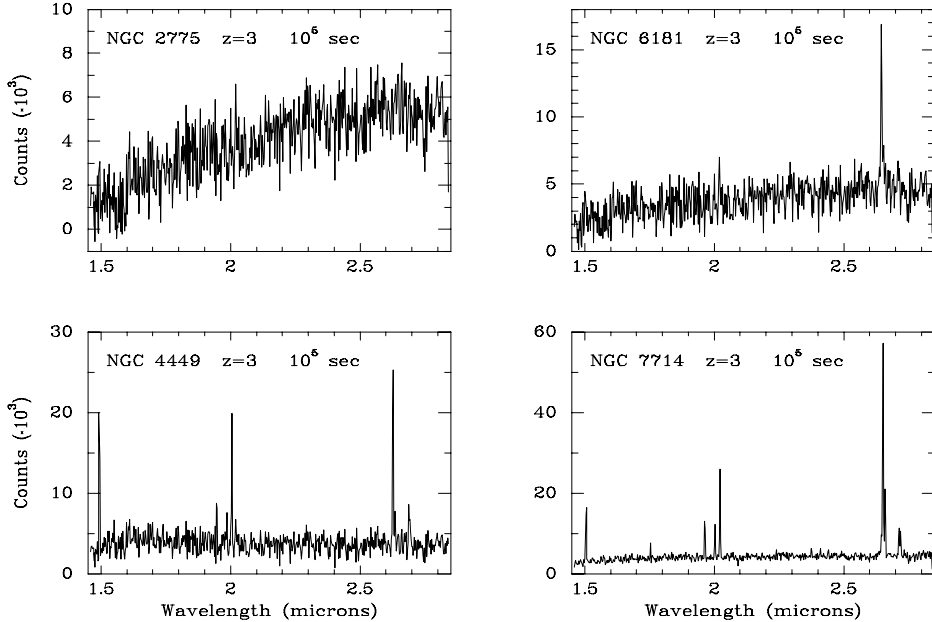


Figure 4. The same galaxies as in Figure 2, but observed at $z = 3$ with NGST, using the parameters in Table 2 and an assumed integration time of 100 ksec. The vertical scale is thousands of counts per channel.

pixels. For NGC 7714 most of the emission is contained in the inner 1 kpc, so I have used a 0.1 arcsec square aperture for this object.

Figure 4 shows that the most useful emission-line spectra will be obtained for galaxies that are analogs to the most active nearby star forming galaxies, such as NGC 4449 and the starburst galaxy NGC 7714. One can expect to detect $H\alpha$ in the analogs to present-day Sb–Sc spirals, but the other diagnostic lines will not be cleanly detected. In the most evolved systems even $H\alpha$ may be absent. However this limitation is less serious than would appear from Figure 4, because galaxies with stellar populations as evolved as those in NGC 2775 and NGC 6181 will be rare above redshifts $z \sim 2$; indeed we already know from groundbased lookback studies that the average emission-line strength in galaxy spectra increases sharply already from $z = 0$ to 1 (e.g., Cowie et al. 1997). If current observations are an accurate indication, emission-line galaxies like NGC 4449 and NGC 7714 will be the dominant population at high redshift, and many of these objects will have luminosities which are more than an order of magnitude higher than the examples shown here.

Another factor that strongly influences the observability of emission-line spectra with NGST is the spatial distribution of the star formation. This is illustrated in Figure 5, which shows simulations of $H\alpha$ monochromatic images of M51, a relatively high surface brightness star forming spiral, and NGC 1222, a merger remnant with a very luminous circumnuclear starburst. The upper panels show $H\alpha$ images of each galaxy, degraded to the 0.03 arcsec pixel sampling of the NGST baseline design (for redshift $z = 2$, but the angular scale is nearly independent of redshift for $z > 1$). The panel sizes are approximately 120 pixels (3.6 arcsec) square for M51, and 60 pixels (1.8 arcsec) for NGC 1222; this illustrates the superb spatial resolution that will be offered by NGST. The lower panels show simulated 100 ksec stacked exposures with NGST for $z = 2$. Although the total SFRs of the two

galaxies are comparable, the emission lines in M51 are barely detectable above $z = 2$, because the star formation is spread over several thousand detector pixels. The signal can be recovered to some extent of course by binning the data, but this eliminates much

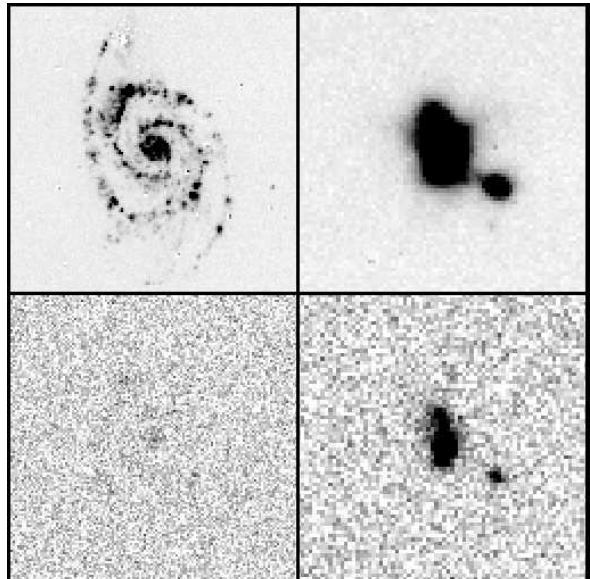


Figure 5. Images showing the distribution of $H\alpha$ emission in M51 (left) and the starburst merger NGC 1222 (right). The upper panels show the galaxies as they are seen locally, but degraded to the spatial resolution of NGST at redshift $z = 2$. The lower panels show the actual detected emission distributions at $z = 2$, for 100 ksec stacked exposures and the instrument parameters given in Table 2. The panel size is roughly 3.6 arcsec (40 kpc) for M51 and 1.8 arcsec (20 kpc) for NGC 1222.

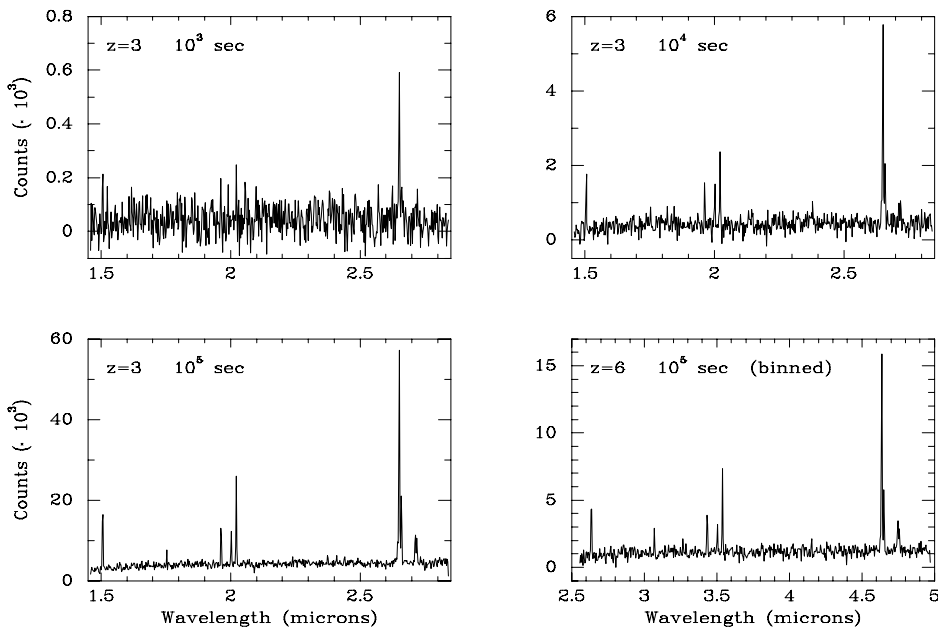


Figure 6. Comparison of spectra of NGC 7714 at $z = 3$, for different total integration times. The bottom right panel shows a spectrum at $z = 6$, with optimized on-chip binning to reduce effective readout noise.

of the advantage of NGST over groundbased applications; indeed a comparable simulation of M51 using a groundbased 8 m telescope (not shown) shows that for resolutions of order a few tenths of an arcsecond the groundbased observations are competitive with NGST shortward of $2 \mu\text{m}$. This is an important lesson, namely that for observations of analogs of local spirals at modest redshifts, much of our information is likely to come from groundbased surveys, and the main contribution of NGST will be to study high surface brightness regions in these galaxies (e.g., their nuclei) at higher spatial resolution.

For compact star forming galaxies (e.g., NGC 1222, NGC 7714), the spatial resolution of NGST is used to full advantage, and simulations show that the bright emission lines can easily be detected in 100 ksec exposures out to $z \geq 9$. Recent HST observations suggest that most of the star formation seen at high redshift in fact takes place in very compact objects, and if this interpretation is correct (i.e., not a consequence of surface brightness bias), then NGC 1222 is the most relevant analog to high- z galaxies, and NGST will easily obtain high S/N spectra of these objects to impressively high redshifts. It is worth noting that most local examples of these luminous starburst galaxies are characterized by very dense dusty star forming regions, so extinction corrections are essential for interpreting the properties of these objects.

The simulations are also useful for exploring the effects of different instrumental tradeoffs on the quality of the spectra. For example Figure 6 compares NGST spectra of NGC 7714 at $z = 3$, for integration times of 1, 10, and 100 ksec. Even for this unusually luminous and compact emission-line galaxy, useful spectral diagnostics require a minimum exposure time of ~ 3 hours, so for applications of this type, integrations of order a day or longer will be needed to make a significant advance over contemporary groundbased surveys. For the parameters used here the exposure times required are tightly linked to the detector noise properties, and reduction in the detector noise could

dramatically lower the exposure times required. This is illustrated in the bottom right panel of Figure 6, which shows a 100 ksec exposure of NGC 7714 at $z = 6$, but with an optimal use of on-chip binning to reduce the readout noise.

Figure 7 shows a similar comparison, but in this case for different spectral resolutions ranging from $R = 100$ to 2500. These are based on identical detector parameters, so they do not include the incremental gain in S/N that can be obtained with on-chip binning at low resolution. However this approximation does not affect the interpretation of the results. Useful information on the strong lines can be obtained down to a limiting resolution of $R = 300 - 400$, but even at this resolution critical diagnostics such as [NII] are lost. Resolutions in the range $R = 800 - 1200$ appear to provide the best balance between resolution and S/N, at least for this particular application.

4. LESSONS AND CONCLUSIONS

I hope that this paper has made a convincing case for the enormous potential that NGST has for reconstructing a comprehensive astrophysical picture of galaxy formation and evolution. There is little doubt that the armada of surveys with 8–10 m telescopes to be carried out over the next decade will provide the basic foundation of this picture, but it remains for NGST to provide the complete set of hard data on galaxy masses, star formation rates, gas and dust contents, chemical abundances, and nuclear properties that will result in a full physical understanding of the origins of galaxies, stars, galactic nuclei, and the chemical elements.

Almost all of this science can be carried out within the NGST baseline capabilities (4–8 m telescope, 1–5 μm wavelength coverage). Exploiting this opportunity, however, imposes instrumental drivers that

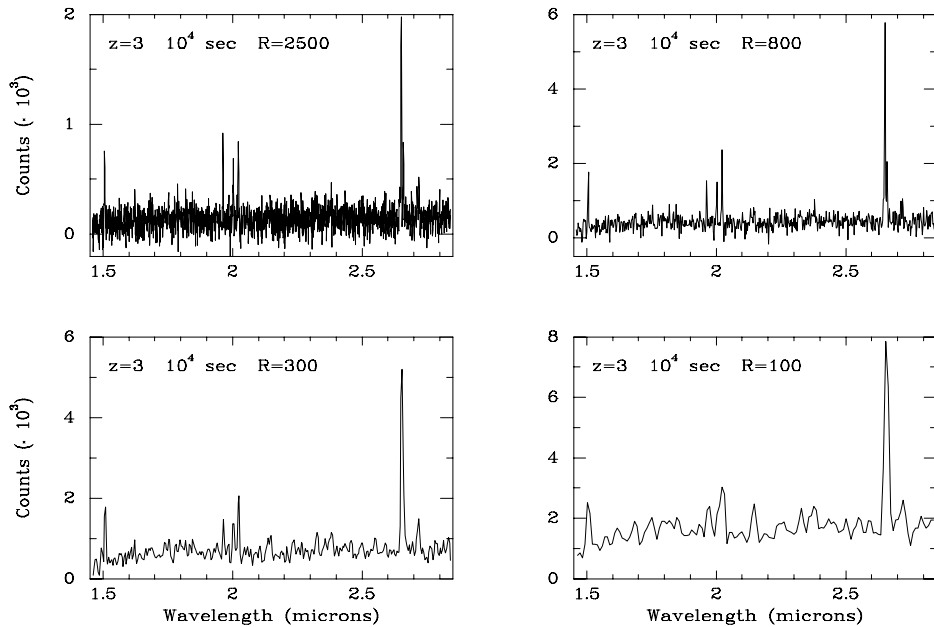


Figure 7. Comparison of spectra of NGC 7714 at $z = 3$, for different spectral resolutions.

may be somewhat more stringent than required by the core mission of redshift surveys of the highest-redshift galaxies. In particular, obtaining diagnostic-quality spectra drives the spectroscopic instrumentation towards resolutions of order 10^3 and signal/noise of order tens. This probably entails typical observing times of order a day (or longer) rather than hours, although this requirement is a direct function of detector noise properties, and improvements in this area would have enormous benefit for all high- z spectroscopic applications. If these needs can be met, the astrophysical payoff promises to be quite extraordinary.

ACKNOWLEDGMENTS

It is a pleasure to acknowledge U of A graduate students Audra Baleisis and Anne Turner for furnishing the $H\alpha$ image of NGC 1222, and undergraduate student James Pizagno for his help with the abundance calculations presented here. I also thank Richard Ellis, Marijn Franx, Garth Illingworth, Chip Kobulnicky, Hans-Walter Rix, Claudia Rola, Matthias Steinmetz, Peter Stockman, and Rodger Thompson for useful discussions about this subject. Some of the work described here is supported by the U.S. National Science Foundation through grant AST-9421145.

REFERENCES

- Bechtold, J., Yee, H.K.C., Elston, R., & Ellingson, E. 1997, *ApJ*, 477, L29
- Buat, V., & Xu, C. 1996, *A&A*, 306, 61
- Calzetti, D., Kinney, A.L., & Storchi-Bergmann, T. 1994, *ApJ*, 429, 582
- Cowie, L.L., Hu, E.M., Songaila, A., & Egami, E. 1997, *ApJ*, 481, L9
- Edmunds, M.G., & Pagel, B.E.J. 1984, *MNRAS*, 211, 507
- Gallagher, J.S., Hunter, D.A., & Bushouse, H. 1989, *AJ*, 97, 700
- Hunter, D.A. 1994, *AJ*, 107, 565
- Kennicutt, R.C. 1983, *ApJ*, 254, 72
- Kennicutt, R.C. 1992a, *ApJ*, 388, 310
- Kennicutt, R.C. 1992b, *ApJS*, 79, 255
- Kennicutt, R.C. 1998, *ARAA*, 36, in press
- Kobulnicky, H.A., Kennicutt, R.C., & Pizagno, J. 1998, in preparation
- Kobulnicky, H.A., & Zaritsky, D. 1998, *ApJ*, in press
- Koo, D.C. et al. 1995, *ApJ*, 440, L49
- Madau, P. et al. 1996, *MNRAS*, 283, 1388
- Martin, C.L. 1997, *ApJ*, 491, 561
- McGaugh, S.S. 1991, *ApJ*, 380, 140
- Pettini, M. et al. 1998, *ApJ*, in press
- Skillman, E.D. 1989, *ApJ*, 347, 883
- Stockman, H.S., ed. 1997, *NGST, Visiting a Time When Galaxies Were Young*, AURA, Inc.
- Veilleux, S., & Osterbrock, D.E. 1987, *ApJS*, 63, 295
- Zaritsky, D., Kennicutt, R.C., & Huchra, J.P. 1994, *ApJ*, 420, 87